Journal of Alloys and Compounds 509 (2011) 3811–3816

Contents lists available at ScienceDirect

Journal of Alloys and Compounds

journal homepage: www.elsevier.com/locate/jallcom

Review

Magnetoelectric $CoFe_2O_4/Pb(Zr_{0.53}Ti_{0.47})O_3$ composite thin films of 2–2 type structure derived by a sol–gel process

Yu-Dong Xu, Guang Wu, Hai-Lin Su*, Min Shi, Gui-Yang Yu, Li Wang

School of Materials Science and Engineering, Hefei University of Technology, Hefei, Anhui 230001, People's Republic of China

ARTICLE INFO

Article history:
Received 15 September 2010
Received in revised form 7 December 2010
Accepted 15 December 2010
Available online 22 December 2010

Keywords:
Magnetic
Ferroelectric
Magnetoelectric
Sol–gel processes
Composite materials

ABSTRACT

$CoFe_2O_4/Pb(Zr_{0.53}Ti_{0.47})O_3$ (CFO/PZT) magnetoelectric composite thin films of 2–2 type structure have been prepared onto $Pt/Ti/SiO_2/Si$ substrate by a sol–gel process and spin coating technique. The optimal annealing process of composite thin films was determined by using X-ray diffraction (XRD) and differential scanning calorimetry (DSC). It is found that the amount of the citric acid and concentration of CFO starting precursor solution have great impact on morphologies of composite thin films. Subsequent scanning electron microscopy (SEM) investigations show that the prepared thin films exhibit good morphologies and compact structure, and cross-sectional micrographs clearly display a multilayered nanostructure of multilayered thin films. The purpose of this work is to determine the optimal annealing processes of composite thin films and to prepare magnetoelectric composite thin films with good microstructure. It is shown that the films exhibit both good magnetic and ferroelectric properties, as well as a magnetoelectric effect.

Contents

1. Introduction

Magnetoelectric (ME) multiferroic materials, which simultaneously exhibit ferroelectricity and ferromagnetism, have recently stimulated increasing interests for their significant potential applications in the next-generation novel multifunctional devices [1–3]. It has been expected that fluctuations in P (polarization) or M (magnetization) can be activated upon applying external magnetic field H or electric field E, respectively. The development of magnetoelectric thin films has become the subject of considerable attention due to their potential applications in microelectromechanical systems [4,5]. Because of a large magnetostrictive coefficient of $CoFe_2O_4$ and a good piezoelectric coefficient of $Pb(Zr_{0.53}Ti_{0.47})O_3$, $CoFe_2O_4/Pb(Zr_{0.53}Ti_{0.47})O_3$ composite thin films have stimulated extensive interests [6–9]. Magnetoelectric thin films have three different nanostructures including 0–3 type, 2–2 type, and 1–3 type. In comparison, it is easier to take control of the growth of horizontal heterostructured (so-called 2–2 type structure) thin films. On the other hand, 2–2 type structure can significantly reduce the leakage current by isolating the low resistive magnetic layers with insulating ferroelectric layers [10]. Therefore, 2–2 type composite thin films have been potential candidates for ME coupling applications.

In this work, $CoFe_2O_4/Pb(Zr_{0.53}Ti_{0.47})O_3$ (CFO/PZT) magnetoelectric composite thin films of 2–2 type heterostructure had been

* Corresponding author. Tel.: +86 0551 2924 380; fax: +86 0551 2924 380.
E-mail address: suhlnju@yahoo.com.cn (H.-L. Su).

0925-8388/$ – see front matter © 2010 Elsevier B.V. All rights reserved.
doi:10.1016/j.jallcom.2010.12.112

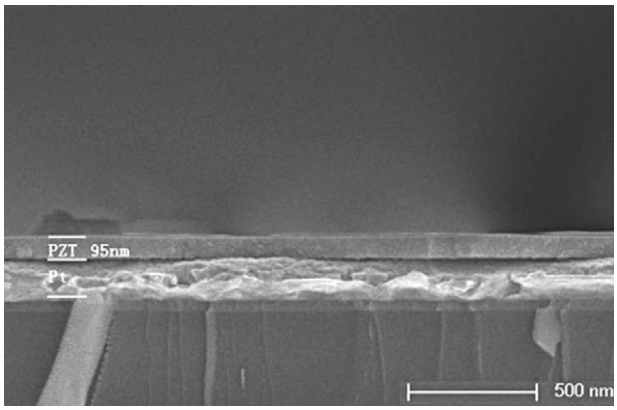

Fig. 1. SEM cross-sectional micrographs of two-layer pure PZT thin films.

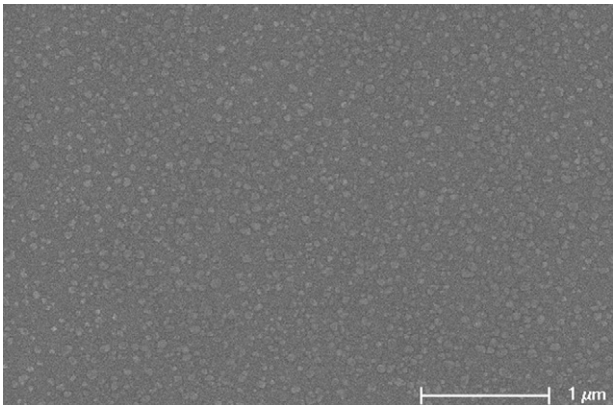

Fig. 2. SEM image of the surface of two-layer pure PZT thin films.

prepared onto Pt/Ti/SiO2/Si substrate by a sol–gel process and spin coating technique. Magnetoelectric composite thin films with good surface and clear interface between two phases were successfully prepared through research on the optimal annealing process of the thin films, concentration of CFO starting precursor solution and amount of the chelating agent (citric acid). X-ray diffraction (XRD Rigaku D/max-RB) with Cu*K*a radiation was used for phase analysis of the films and powders. Scanning electron microscopy (SEM, Hitachi S5500) was used for observation of the film microstructure. Differential scanning calorimetry (DSC, NETZSCH 404 C) was used to analyze the thermal behavior of PZT and CFO powders. Vibrating sample magnetometer (VSM, Lakeshore, Model 7300 series) was used to characterize the magnetic properties of the films. The ferroelectric measurements were performed using a Radiant Technologies Precision Workstation ferroelectric test system. ME effects of the films were measured using a ME measuring device.

2. Experimental

2.1. Preparation of PZT starting precursor solution and thin films

The appropriate portions of zirconium nitrate pentahydrate ($Zr(NO_3)\cdot 5H_2O$) and tetrabutyl titanate ($Ti(C_4H_9O)_4$) were dissolved in 2-methoxyethanol, respectively. Lead acetate trihydrate ($Pb(CH_3COO)_2\cdot 3H_2O$) was dissolved in acetic acid. Before lead acetate trihydrate and tetrabutyl titanate solution were mixed, appropriate amount of acetylacetone was added into tetrabutyl titanate solution to prevent the formation of precipitation. Then, zirconium nitrate pentahydrate solution was added into above solution and stirred at 80 °C to form PZT starting precursor solution of 0.3 mol/L. The molecule ratio of Pb:Zr:Ti was 1.1:0.53:0.47. Lead acetate trihydrate with additional 10 mol% was added into the solution to compensate the lead loss during annealing process.

The PZT starting precursor solution was spin coated onto the Pt/Ti/SiO2/Si substrate at a spinning rate of 3200 rpm for 30 s. Then, the gel film was successively dried at 150 °C for 2 min and pre-annealed at 350 °C for 2 min. This spin-coating/drying procedure was repeated several times until the required thickness of the films. Finally, the film was annealed at 650 °C for 10 min by a rapid annealing process. Fig. 1 shows SEM cross-sectional micrographs of two-layer PZT thin films (thickness of each layer is about 40 nm). Fig. 2 shows SEM image of the surface of above-mentioned PZT films. The results reveal that the films are crack-free and have compact structure without any pore.

2.2. The preparation of CFO starting precursor solution and thin films

The appropriate portions of iron nitrate ($Fe(NO_3)_3$), cobalt nitrate ($Co(NO_3)_2$), citric acid, $C_6H_8O_7$, were dissolved in ethanol, respectively. Solution of iron nitrate and cobalt nitrate was first mixed together, then added citric acid solution into above solution and stirred continuously to form a CFO starting precursor solution. The molecule ratio of Co:Fe:$C_6H_8O_7$ can be 1:2:3 or 1:2:6. The preparation of pure CFO thin films was similar to PZT.

2.3. The preparation of CFO/PZT magnetoelectric composite thin films

Firstly, the PZT starting precursor solution was spin coated onto the Pt/Ti/SiO2/Si substrate and dried. This spin-coating/drying procedure was repeated two times, and then two-layer PZT thin films were annealed at 650 °C for 10 min by a rapid annealing process. After that, the CFO starting precursor solution was spin coated onto the PZT films and dried, and this procedure was repeated four times. Finally, the composite thin films were annealed at 650 °C for 10 min by a rapid annealing process. The composite thin films were prepared by repeating the above process, which structure is substrate/2PZT/4CFO/2PZT/4CFO.

3. Results and discussion

3.1. The optimal annealing process of composite thin films

The PZT and CFO starting precursor solution were successively dried at 120 °C for 30 min, and then ball milled for 10 h. Thus PZT and CFO powders were finally obtained. DSC curve of PZT powders is shown in Fig. 3. It can be found from Fig. 3 that the peak at 150 °C was attributed to the evaporation of organic solvent, the decomposition and combustion of the bound organic species in the powders contributed to the exothermic peaks before 450 °C. The peak around 650 °C indicated the formation of the perovskite phase. Based on the DSC result, the drying temperature of PZT thin films was chosen at 150 °C.

However, it should be noticed that degree of crystallization of PZT thin films also has a great influence on the growth of the final composite thin film products, because PZT films were first deposited on the substrate. Fig. 4 shows XRD results of PZT thin films at four different pre-annealing temperatures (thin films were finally annealed at 650 °C). From the results it can be found that the PZT thin films have bad crystallinity when the preparatory annealing temperature is at 300 °C. However, most intense PZT phase peaks can be found in XRD spectrum when pre-annealing tem-

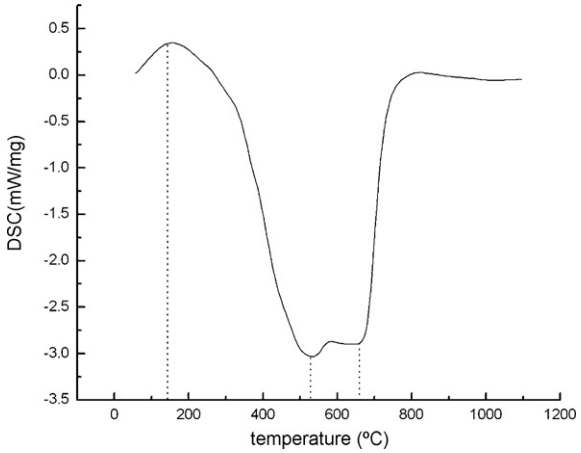

Fig. 3. DSC curve of PZT powders.

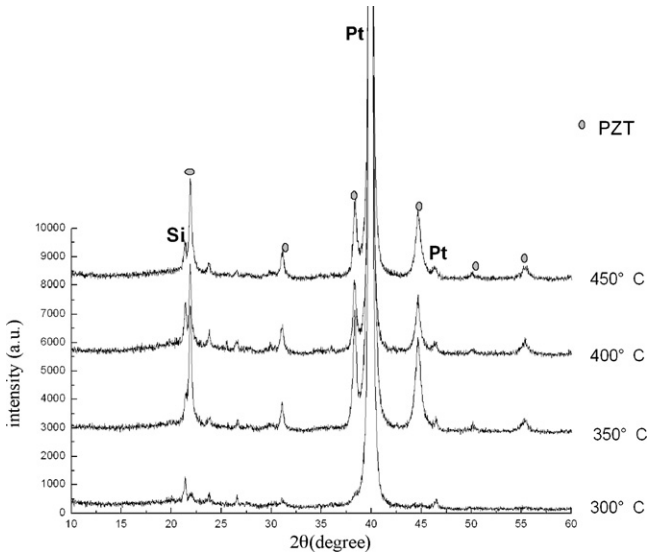

Fig. 4. XRD results of PZT thin films pre-annealed at different temperatures, all of these films were finally annealed at 650 °C.

perature reaches 350 °C. Consequently, the optimal pre-annealing temperature should be at 350 °C. Fig. 5 shows XRD results of PZT powders annealed at different temperatures by a rapid annealing process. It is apparent that there is no any other detectable impurity phase when the temperature is increased to 650 °C. Consequently, the lowest annealing temperature of PZT thin films was chosen at 650 °C. In summarizing, the optimal annealing process of PZT films is as follows: firstly dried at 150 °C, then pre-annealed at 350 °C and finally annealed at 650 °C.

Fig. 6 shows DSC curve of CFO powders. The peak at 120 °C was attributed to the ethanol evaporation. Decomposition and combustion of the bound organic species occurred at the temperatures from 120 °C to 320 °C. After the peak at 400 °C, it indicated the formation of the spinel phase. Fig. 7 shows XRD results of CFO powders annealed at two different temperatures. There is only CFO phase when the temperature is increased to 550 °C. Based on the DSC and XRD results, drying steps of CFO thin films at 120 °C and 320 °C were chosen, and the lowest annealing temperature of CFO thin films can be at 550 °C.

From the above results, PZT and CFO thin films were annealed at 650 °C and 550 °C to assure the formation of pure phase, respectively. The lowest annealing temperature of PZT thin films was higher than that of CFO. So, the lowest annealing temperature of composite thin films was chosen at 650 °C to ensure formation of pure PZT and CFO phase, and the same annealing temperature of PZT and CFO was also beneficial to prevent the component diffusion between two phases. Fig. 8 shows XRD results of CFO/PZT composite thin films annealed at 650 °C. All peaks can be identified, and there are no additional or intermediate phase peaks apart from CFO and PZT.

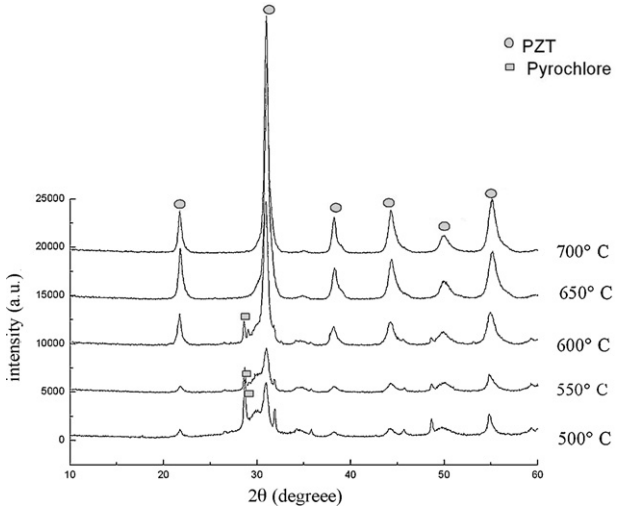

Fig. 5. XRD results of PZT powders annealed at different temperatures.

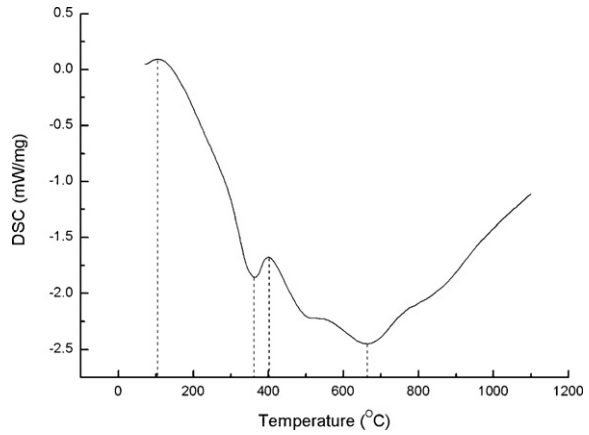

Fig. 6. DSC curve of CFO powders.

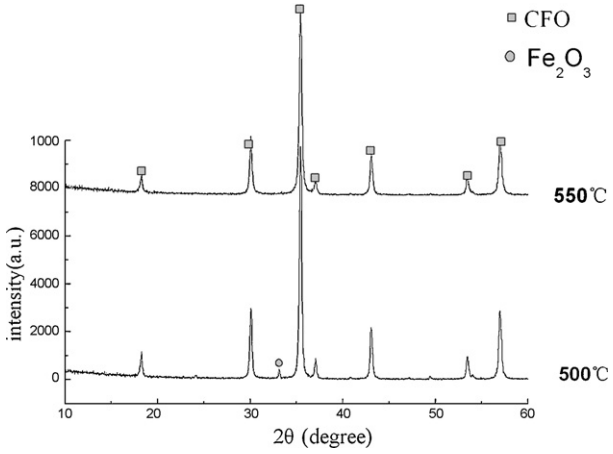

Fig. 7. XRD results of CFO powders annealed at different temperatures.

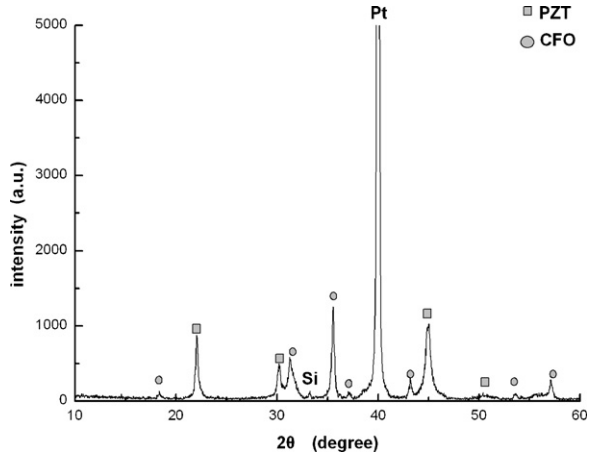

Fig. 8. XRD results of CFO/PZT composite thin films annealed at 650 °C.

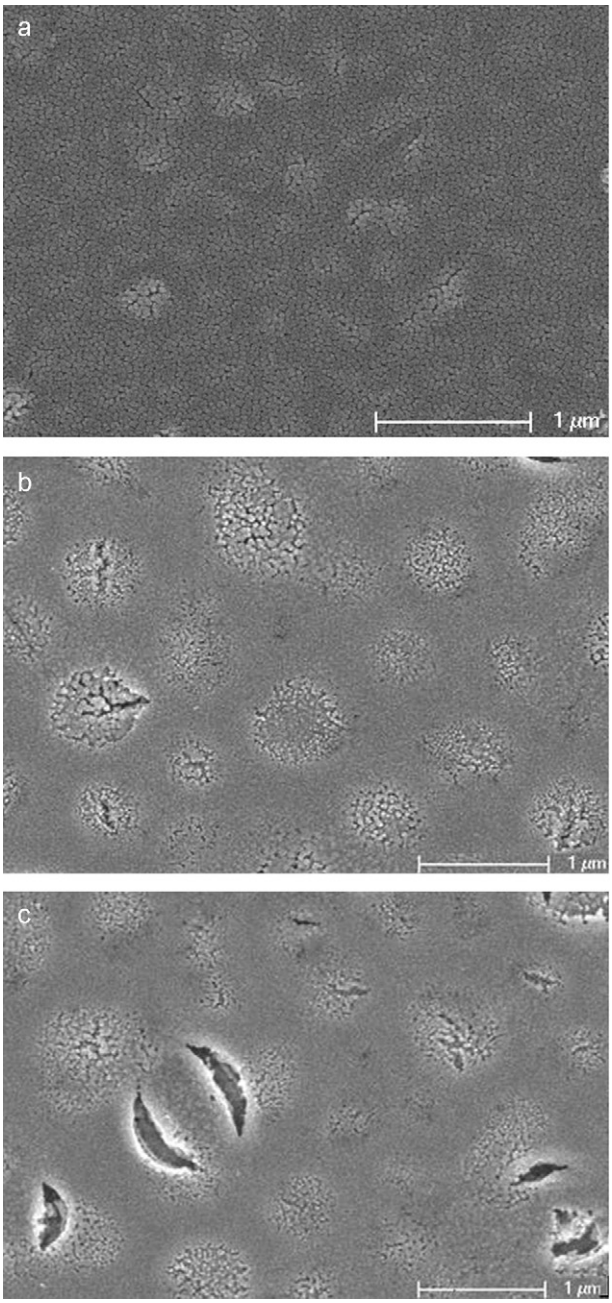

Fig. 9. SEM images of the surface of CFO thin films prepared by three different concentrations of CFO starting precursor solution. (a) 0.1 mol/L, (b) 0.2 mol/L, and (c) 0.3 mol/L.

3.2. Characterization of microstructure of composite thin films

Citric acid and the concentration of CFO starting precursor solution had an impact on morphologies of CFO thin films which led to changes in morphologies and thickness of composite thin films. Fig. 9 shows SEM images of surfaces of CFO thin films prepared by different concentrations of CFO starting precursor solution. Based on the SEM results, it can be seen that decreasing concentration of the solution can significantly reduce cracks of the films. When the concentration of CFO starting precursor solution was 0.1 mol/L, the CFO film is crack-free. Composite thin films were prepared using different concentrations of CFO starting precursor solutions (0.1 mol/L and 0.3 mol/L), which structure is substrate/2PZT/4CFO/2PZT/4CFO. Figs. 10 and 11 show the SEM cross-sectional micrographs of composite thin films. When the concentration of CFO starting precursor solution is 0.1 mol/L, the composite films are crack-free and have a compact structure without any pore. Otherwise, the surface of composite thin films is rough and cross-sectional micrographs do not display the multilayered nanostructure when the concentration of CFO starting precursor solution is 0.3 mol/L. This can be explained by the large stress in films during annealing process. In fact, each layer of CFO thin films was thicker resulting in larger stress in the films when the concentration of CFO starting precursor solution was high. Undoubtedly, composite thin films with better morphologies can be prepared by selecting appropriate concentrations of CFO starting precursor solution.

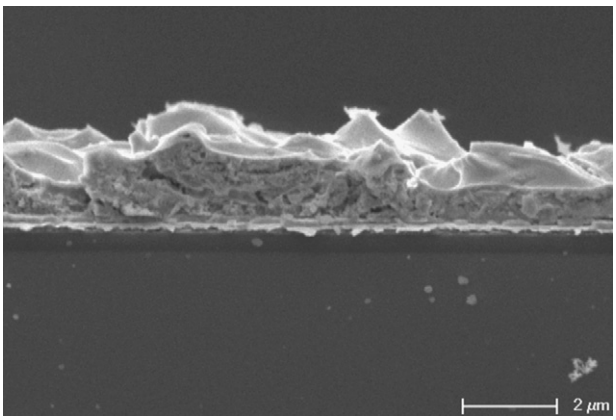

Fig. 10. SEM cross-sectional micrograph of composite thin films, the concentration of CFO starting precursor solution is 0.3 mol/L, Co:citric acid = 1:6.

Figs. 11 and 12 show SEM cross-sectional micrographs of composite thin films prepared using CFO starting precursor solution with different molecule ratios of Co and citric acid (Co:citric acid = 1:6, 1:3). Based on the SEM images, the thickness of CFO films increased from about 130 nm to 200 nm when the ratio of Co and citric acid changed from 1:3 to 1:6. It can also be found that a more flat cross-section and more uniform distribution of thickness of composite films are observed when the citric acid content changed. In general, the role of citric acid is to act as a chelating agent to form a uniform and stable CFO starting precursor solution. That is to say, combination of citric acid ionized $COOH^-$ and complex ions of Fe^{3+} and Co^{2+} is proved to exhibit an important impact on the uniformity of chemical components and final thin film products.

From above results it can be concluded that the prepared 2–2 type magnetoelectric composite films (PZT/CFO) exhibit relatively

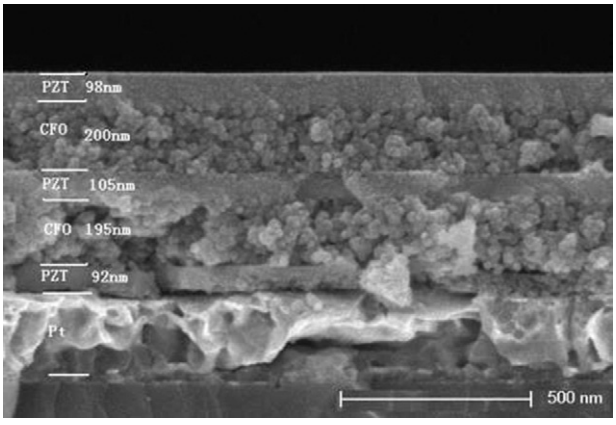

Fig. 11. SEM cross-sectional micrograph of composite thin films, the concentration of CFO starting precursor solution is 0.1 mol/L, Co:citric acid = 1:6.

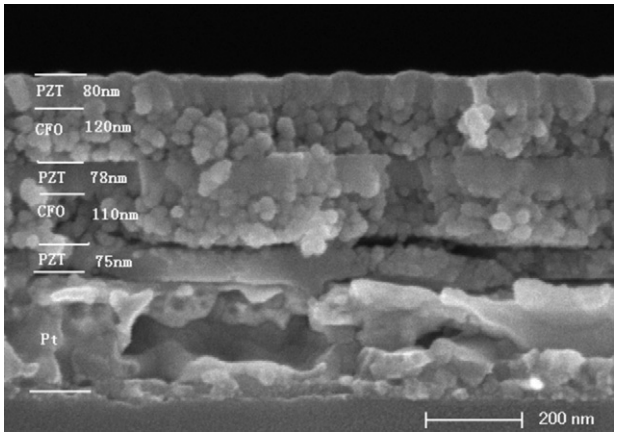

Fig. 12. SEM cross-sectional micrograph of composite thin films, the concentration of CFO starting precursor solution is 0.1 mol/L, Co:citric acid = 1:3.

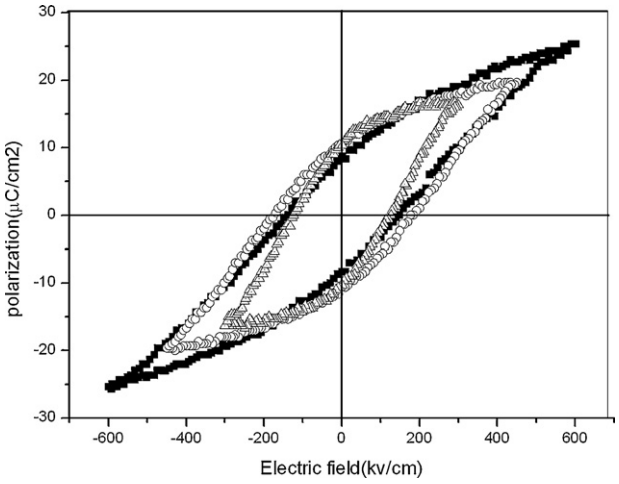

Fig. 14. *P–E* hysteresis loops of the composite thin films.

better morphologies and the layered structure of films are more clearly visible compared with some other corresponding results. Except sol–gel process there are other methods used to prepare magnetoelectric composite thin films such as pulsed laser deposition (PLD). Single-crystal composite films were prepared with much better morphologies by using PLD process, respectively [11–13]. But the PLD process is very expensive and not helpful to cost savings compared with sol–gel process.

3.3. Characterization of magnetoelectric properties of composite thin films

A vibrating sample magnetometer was used to characterize the magnetic properties of films with better morphologies as shows in Fig. 11. The field dependent magnetizations were measured at room temperature by applying magnetic fields perpendicular or parallel to the plane of the films. Fig. 13 shows the magnetic hysteresis loops for the films. The saturation magnetizations of the in-plane and out-of-plane loops show 298 and 272 emu/cm^3, the composite films show relatively large values compared with some other corresponding results. Both in-plane and out-of-plane loops have similar shapes, and the coercivity H_c of the composite thin films is the same for both loops, this means although there are indeed signs of shape anisotropy in these hysteresis, they are masked by the very large magnetocrystalline anisotropy of CFO.

Pt electrode dots with 0.2 mm in diameter were deposited on the composite films surface for ferroelectric measurement. Fig. 14 shows the ferroelectric *P–E* curves of films at room temperature under the applied voltage. The maximum voltage is in the range of 300–600 kV/cm. The well-defined ferroelectric loops are observed, and the saturation polarization (P_s) and remanent polarization (P_r) reach 25.3 and 8.3 μC/cm^2 at E = 600 kV/cm. The polarization values for the composite films are lower than those pure PZT films prepared by the same processing (P_r = 18.5 μC/cm^2 and P_s = 41.1 μC/cm^2) [10]. Because of the existence of ferromagnetic CFO layers in composite films, the ferroelectric properties can be effected [14].

The magnetoelectric voltage coefficient $\alpha_E = dE/dH$, which is characterized by the induced electric field E under an applied ac magnetic field H (9 V) generated by a pair of Helmholtz coils, was then measured as function of dc magnetic bias H_{Bias} for the composite thin films. Both of ac magnetic field and dc magnetic field were superimposed and parallel to the film plane. Frequency of the voltage signal applied on Helmholtz coils was 50 kHZ. Fig. 15 shows the variation of αE with H_{Bias} at an ac magnetic frequency of f = 50 kHz. It is clear that the composite thin films exhibit significant magnetoelectric effect which depends on H_{Bias}. The maximum α_E value of 273 mV/cm was obtained at initial H_{Bias}, which is larger than that of the bulk ferroelectric–ferromagnetic composite [15,16]. It is also comparable with some other corresponding results of composite films in the literature [17].

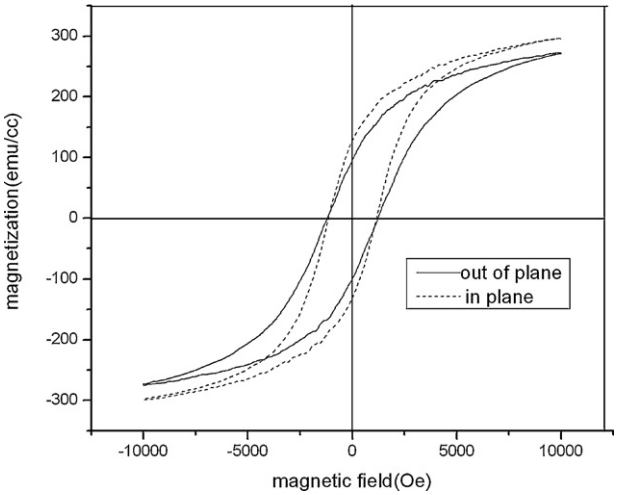

Fig. 13. Magnetic hysteresis loops of the composite thin films.

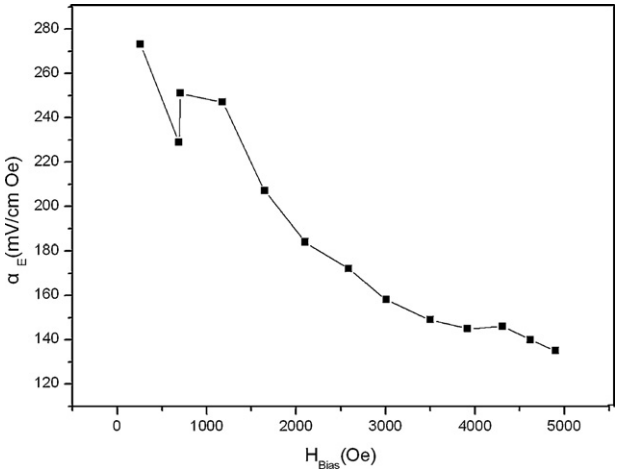

Fig. 15. Variations of α_E with H_{Bias} for the composite thin films.

4. Conclusion

$CoFe_2O_4/Pb(Zr_{0.53}Ti_{0.47})O_3$ (CFO/PZT) magnetoelectric composite thin films of 2–2 type heterostructure have been prepared onto Pt/Ti/SiO2/Si substrate by a sol–gel process and spin coating technique. Structure of composite thin films is substrate/2PZT/4CFO/2PZT/4CFO. Optimal annealing processes of composite thin films have been studied. Amount of the citric acid and concentration of CFO starting precursor solution have been determined. The finally prepared composite thin films have good surface and a compact structure without any pore, and the composite thin films also exhibit good magnetic and ferroelectric properties, as well as a magnetoelectric effect.

Acknowledgement

This work was supported by the Specialized Research Fund for the Doctoral Program of Higher Education (Grant No. 200803591037).

References

[1] W. Eerenstein, N.D. Mathur, J.F. Scott, Nature 442 (2006) 759.
[2] M. Fiebig, J. Phys. D: Appl. Phys. 38 (2005) R123.
[3] R.C. Kambalea, P.A. Shaikha, C.H. Bhosalea, K.Y. Rajpurea, Y.D. Kolekarb, J. Alloys Compd. 310 (2010) 489.
[4] H.M. Zheng, J. Kreisel, Y.H. Chu, R. Ramesh, L. Salamanca-Riba, Appl. Phys. Lett. 90 (2007) 113113.
[5] M. Kumar, K.L. Yadav, J. Phys. Chem. Solids 68 (2007) 1791.
[6] N. Ortega, P. Bhattacharya, R.S. Katiyar, D. Putta, A. Manivannan, M.S. Seehra, I. Takeuchi, S.B. Majumder, J. Appl. Phys. 100 (2006) 126105.
[7] S.H. Xie, J.Y. Li, Y. Qiao, Y.Y. Liu, L.N. Lan, Y.C. Zhou, S.T. Tan, Appl. Phys. Lett. 92 (2008) 062901.
[8] H.C. He, J.P. Zhou, J. Wang, C.W. Nan, Appl. Phys. Lett. 89 (2006) 052904.
[9] J.G. Wan, H. Zhang, X.W. Wang, D.Y. Pan, J.M. Liu, G.H. Wang, Appl. Phys. Lett. 89 (2006) 122914.
[10] H.C. He, J. Wang, B.P. Zhou, C.W. Nan, Adv. Funct. Mater. 17 (2007) 1333.
[11] C.Y. Deng, Y. Zhang, J. Ma, Y.H. Lin, C.W. Nan, Acta Mater. 56 (2008) 405.
[12] J. Ryu, S. Priya, J. Ceram. Sci. 84 (12) (2001) 2095.
[13] J.P. Zhou, H.C. He, Z. Shi, C.W. Nan, Appl. Phys. Lett. 88 (2006) 013111.
[14] S.Z.A.L. Royturd, S.P. Alpay, Appl. Phys. Lett. 87 (2005) 092902.
[15] J. van den Boomgaard, R.A.J. Born, J. Mater. Sci. 13 (1978) 1538.
[16] J. van den Boomgaard, A.M.J.G. Van Run, J. Van Suchetelene, Ferroelectrics 10 (1976) 295.
[17] J.G. Wan, X.W. Wang, Y.J. Wu, M. Zeng, Y. Wang, H. Jiang, W.Q. Zhou, G.H. Wang, J.M. Liu, Appl. Phys. Lett. 86 (2005) 122501.